THERMAL EFFECTS OF LASER RADIATION IN BIOLOGICAL TISSUE

LARIMORE CUMMINS
Dominican Santa Cruz Hospital, Santa Cruz, California 95065

MICHAEL NAUENBERG
Institute for Theoretical Physics, University of California, Santa Barbara, California 92106

ABSTRACT A theoretical model is presented that simulates the thermal effects of laser radiation incident on biological tissue. The multiple scattering and absorption of the laser beam and the thermal diffusion process in the tissue are evaluated by a numerical technique that is well suited for microcomputers. Results are compared with recent empirical observations.

INTRODUCTION

The thermal effects of laser radiation have been studied in many ways. Medical applications of lasers have focused particular interest on the interaction of infrared laser light in biological tissue (1–3). For several years, lasers have been used to repair damaged retinae, thus preventing blindness. More recently, lasers have been used by surgeons to cut into tissues (carbon dioxide laser scalpel), to stop internal hemorrhage (Neodymium:YAG and Argon laser photocoagulation) and to treat tumors (1, 4, 5). Although the clinical applications of lasers are rapidly multiplying, it still is not clear how the laser exerts its effects. The physical heterogeneity of biological tissue results in considerable regional variation in light absorption and scattering, two of the critical processes that determine the pattern of heating. The effects of this heterogeneity are poorly understood. Furthermore, the effects of multiple scattering of the incident laser beam, which play a dominant role in the case of the Neodymium:YAG (Nd:YAG) laser, have not been properly taken into account in previous works (6–10).

In this study we have developed a numerical technique to consider the classic problem of light scattering, light absorption, and thermal diffusion, which allows for spatial and temperature-dependent variation of these events. Such spatial variables include the presence of pigment, tissue organelles, and blood vessels. Associated with these structures are variations in light absorption and scattering as well as heat transfer. Temperature-dependent variables are related to the physical changes that tissue undergo during heating, including coagulation, carbonization, and vaporization. Our method is to represent the tissue as a lattice of finite cells using difference equations, which are readily amenable to numerical techniques, instead of differential equations. These equations can be solved with the use of commonly available microcomputers that permit convenient graphical display of the pertinent variables. We present the results of several computations that were carried out on a Hewlett-Packard Co.(Palo Alto, CA, model 9845B) desk top computer, and we compare these results with recent empirical observations.

MULTIPLE SCATTERING APPROXIMATION

In this section we develop an approximate treatment for multiple scattering of the laser beam inside tissue, which plays an essential role in the case of the Nd:YAG laser. Some of the previous studies have applied a single scattering formula, but they used a scattering coefficient 100 times larger than the absorption coefficient, which is inconsistent with the single scattering assumption (7–10). An alternative approach to multiple scattering has been applied by Langerholc (11).

Let $I(r, \hat{\mathbf{n}})$ be the total intensity of radiation along the direction represented by the unit vector $\hat{\mathbf{n}}$ at the position r inside the tissue, which is produced by a laser beam incident on the surface of the tissue. The change in the intensity due to the combined effect of absorption and scattering is determined by a differential equation, which, for isotropic scattering, takes the form (12)

$$n \cdot \Delta I(r, \hat{\mathbf{n}}) = [\alpha(r) + \beta(r)]I(r, \hat{\mathbf{n}}) + \beta/4\,(r) \int d\Omega'\, I(r, \hat{\mathbf{n}}'). \quad (1)$$

The integral is over the solid angle subtended by $\hat{\mathbf{n}}'$, and $\alpha(r)$ and $\beta(r)$ are the absorption and scattering coefficients, respectively, that may depend on r. The appropriate boundary conditions for a laser beam incident on a tissue of finite thickness specifies the intensity $I(r, n)$ at the surfaces of the tissue, and will be described later.

We will approximate the solution of Eq. 1 by replacing the integral over solid angle by a sum over finite directions n, and by introducing a finite lattice of points that allows us to replace the derivatives by finite differences. The resulting equations can then be solved numerically with the aid of a digital computer.

For the case of cylindrical symmetry, the simplest approximation is to include only the radiation $I(r, \pm\hat{\mathbf{z}})$ along and opposite the laser beam

Dr. Nauenberg's present address is the University of California, Santa Cruz, CA 95064.

direction, which has been chosen as the z-axis, and the radiation $I(r, \pm\hat{\mathbf{r}})$ in the directions perpendicular to this axis. Setting $z_i = i\Delta z$ and $r_j = j\Delta r$, where $i = 0, 1, \ldots M$, $j = 0, 1 \ldots N$, and $\Delta z = D/M$, $\Delta r = R/N$, where D is the thickness and R is the radius of the tissue, we have

$$I(i+1, j; +\hat{\mathbf{z}}) = [1 - (\alpha+\beta)\Delta z]\, I(i, j; +\hat{\mathbf{z}}) + \beta/4\, \Delta z\, I(i, j)$$

$$I(M-i-1, j; -\hat{\mathbf{z}}) = [1 - (\alpha+\beta)\Delta z] \cdot I(M-i, j; -\hat{\mathbf{z}}) + \beta/4\Delta z\, I(i, j)$$

$$I(i, j+1; +\hat{\mathbf{r}}) = [1 - (\alpha+\beta)\Delta r]\, I(i, j; +\hat{\mathbf{r}}) + \beta/4\, \Delta r\, I(i, j)$$

$$I(i, N-j-1; -\hat{\mathbf{r}}) = [1 - (\alpha+\beta)\Delta r] \cdot I(i, N-j; -\hat{\mathbf{r}}) + \beta/4\, \Delta r\, I(i, j) \quad (2)$$

where $I(i, j) = I(i, j; +\hat{\mathbf{z}}) + I(i, j; -\hat{\mathbf{z}}) + I(i, j; +\hat{\mathbf{r}}) + I(i, j; -\hat{\mathbf{r}})$ is the total radiation intensity at z_i, r_j. This approximation can be readily improved by adding the contributions from other scattering angles, which provides also an estimate of the error made in Eq. 2 .

In this approximation the boundary conditions for Eq. 2 take the simple form

$$I(0, j; +\hat{\mathbf{z}}) = L(j)$$

$$I(M, j; -\hat{\mathbf{z}}) = I(i, 0; +\hat{\mathbf{r}}) = I(i, N; -\hat{\mathbf{r}}) = 0 \quad (3)$$

where $L(j)$ is the incident laser beam intensity.

It is straightforward to solve these equations numerically by an iterative process. For a laser beam with a Gaussian profile set $L(j) = L_0 e^{-(j\Delta r/r_0)^2}$ where r_0 is the radius of the beam. To evaluate Eq. 2 initially, set $I(i, j; -\hat{\mathbf{z}}) = I(i, j; +\hat{\mathbf{r}}) = I(i, j; -\hat{\mathbf{r}}) = 0$ on the right-hand side. The result is then substituted back in Eq. 2 together with the boundary conditions, Eq. 3, to obtain a second approximation solution to Eq. 2. This procedure is repeated until the solutions do not change further within a prescribed accuracy. In practice it turns out that this iteration procedure converges very rapidly.

HEAT DIFFUSION

To evaluate the diffusion of heat produced in the tissue by the absorption of the laser radiation, we will also approximate the familiar differential equations for heat transport by difference equations. In particular this method will allow us to include changes in the thermal diffusivity and specific heat that depend on the local temperature as well as on structural heterogeneity within the tissue.

Let $T(i, j; k)$ be the temperature in the i, j cell at time $t_k = k\Delta t$, where Δt is a small time differential and k is an integer $k = 0, 1, 2\ldots$. The heat flux in the radial direction, $J_r(i, j; k)$, between cells i, j and $i, j+1$, and the corresponding flux in the axial direction $J_z(i, j; k)$ between cells i, j and $i+1, j$ is then given by

$$J_r(i, j; k) = -2/(\Delta r)\, [T(i, j+1; k) - T(i, j; k)] / [H^{-1}(i, j+1; k) + H^{-1}(i, j; k)]$$

$$J_z(i, j; k) = -2/(\Delta z)\, [T(i+1, j; k) - T(i, j; k)] / [H^{-1}(i+1, j; k) + H^{-1}(i, j; k)] \quad (4)$$

where $H(i, j; k)$ is the heat diffusivity. Note that $H(i, j; k)$ may depend on the temperature or time as well as the composition of the i, j cell.

The temperature at the i, j cell at the later time $t_{k+1} = (k+1)\,\Delta t$ is then determined by the relation

$$T(i, j; k+1) = T(i, j; k) - \frac{\Delta t}{\Delta r}\left[J_r(i, j; k)\left(1 + \frac{1}{2j}\right) - J_r(i, j-1; k) \cdot \left(1 - \frac{1}{2j}\right)\right] - \frac{\Delta t}{\Delta z}\,[J_z(i, j; k) - J_z(i-1, j; k)] + \frac{\alpha(i, j)}{C(i, j)}\, I(i, j) \quad (5)$$

where $I(i, j)$ is the intensity of radiation at the i, j) cell which we discussed in the previous section, and $C(i, j)$ is the specific heat.

The appropriate boundary conditions for Eq. 5 are vanishing radial heat flux at the center of the tissue $J_r(i, 0; k) = 0$, and

$$T(0, j) = T(M+1, j) = T(i, N+1) = T_0 \quad (6)$$

where T_0 is the temperature of the medium (air) surrounding the tissue. Likewise,

$$H(0, j) = H(M+1, j) = H(i, N+1) = H_0 \quad (7)$$

where H_0 is the heat diffusivity of the surrounding medium.

Again, it is straightforward to obtain the temperature at any location i, j in the tissue at time $t_k = k\,\Delta\, t$ by evaluating numerically with the aid of a computer the recursion relations defined by Eqs. 4–6. Several such calculations will be discussed in the next section.

RESULTS

Based on the above theoretical treatment, we present in this section some of the results that have been obtained by solving the foregoing equations numerically, and compare these with recent empirical observations. Computations were carried out on the Hewlett-Packard model 9845B desk top computer.

Halldorsson et al. (8) have measured the pattern of heating of bloodless dog and human tissue in response to the Nd:YAG laser radiation at a wavelength of 1.06 μm. Fig. 1 compares the theoretical and observed temperatures as a function of time when a 2-mm thick section of canine stomach is irradiated using a power setting of 50 W distributed over a circular area of 3 mm diam (spot size). The laser is turned off after 4 s allowing both heating and cooling phenomena to be compared with theory. Both front (irradiated) and back surface temperature of the tissue are measured. Halldorsson (7) measured tissue temperature with a scanning infrared thermal camera. The theoretical values derived from the current model provide a reasonably close fit. Values for absorption and scattering coefficients have yet to be experimentally determined. Reported estimates vary considerably (1, 4, 5, 8, 13). The current model should provide a theoretical basis for more precise determination. For purposes of this study we have assumed the scattering coefficient to range between one and two orders of magnitude greater than the absorption coefficient for

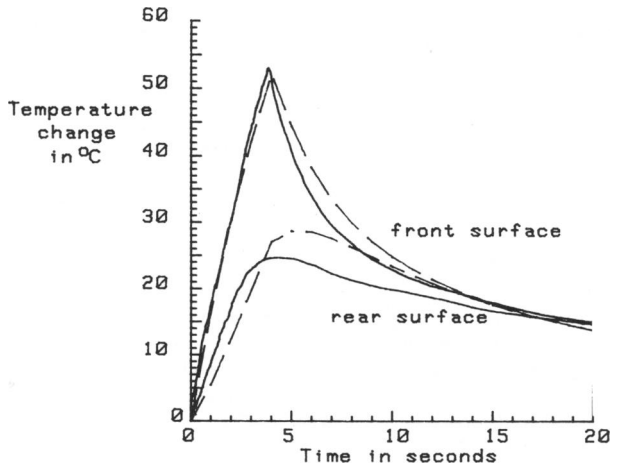

FIGURE 1 Heating of a 2-mm thick section of bloodless mammalian tissue using the Nd:YAG laser at a power setting of 40 W, spot size of 3 mm and pulse duration of 4 s. Measured values are from Halldorsson et al. (8), (—). The following values were used to calculate theoretical temperatures, (---·): absorption coefficient (α) = 0.085 cm^{-1}, scattering coefficient (β) = 10 cm^{-1}, thermal conductance constant (C) = 0.0015 cm^2/s, and boundary condition for thermal diffusion (B) = 1/80, where B is a fraction of thermal conductance.

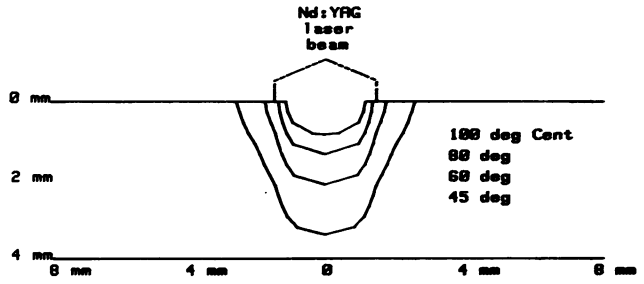

FIGURE 3 Theoretical heating pattern within mammalian tissue with a baseline temperature of 37°C using the Nd:YAG laser at a power setting of 80 W, spot size of 3-mm, after a single pulse duration of 1.5 s.

Nd:YAG laser (1, 5, 7). These coefficients are assumed to be approximately equal for the Argon laser (4, 5). For the CO_2 laser we have assumed the scattering to be nonexistent (8, 5). The best fit values for the Nd:YAG laser are as listed in Fig. 1. Fig. 2 demonstrates the sensitivity of the current model to variations in absorption and scattering, as well as heat diffusion. These values represent coefficient variations well within the range expected for biological tissues. Changes in mathematical boundary conditions represent a realistic variation such as the air-filled stomach vs. the water-filled urinary bladder.

There are as of yet no published observations of temperature within biological tissue undergoing laser heating. Fig. 3 describes the theoretical distribution of temperatures within such tissue. The data are presented as isothermal lines for 40°, 60°, 80°, and 100°C starting with a preirradiation temperature of 37°C. Protein coagulation and immediate tissue necrosis occur at 60°C. Therefore, the 60°C isotherm represents the minimal distribution of coagulated tissue immediately after laser irradiation. Such

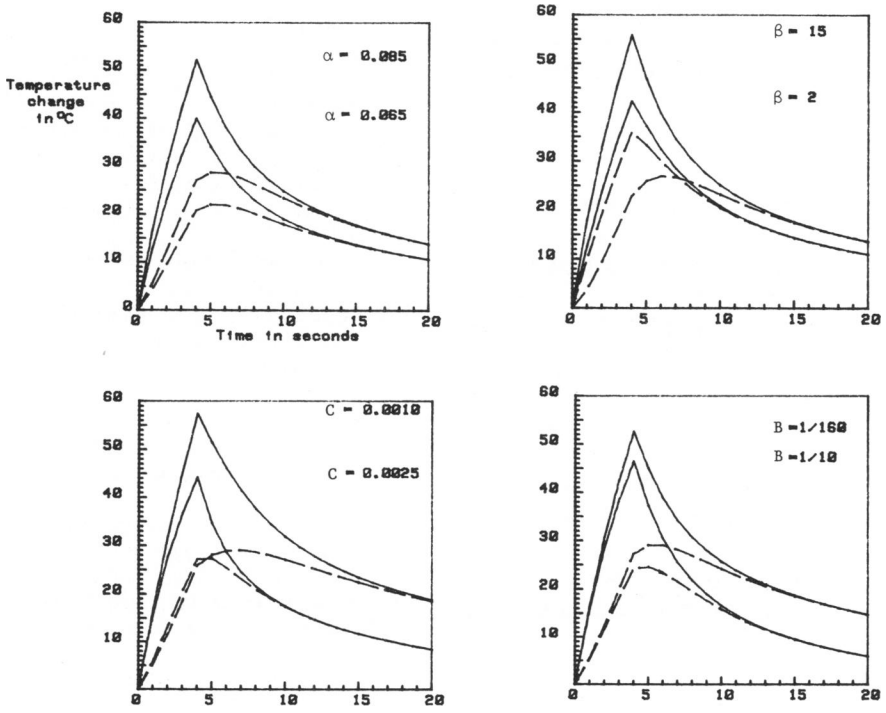

FIGURE 2 Theoretical heating of tissue as in Fig. 1. Coefficients of absorption (α), scattering (β), thermal conductance constant (C), and boundary conditions for thermal diffusion (B) are varied as noted. Unless otherwise indicated the values are the same as in Fig. 1. Plotted are front wall (—) and rear wall (---) temperatures.

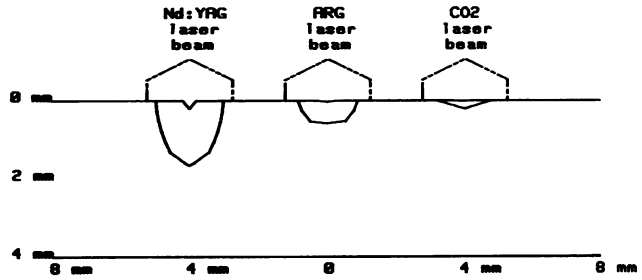

FIGURE 4 Theoretical heating pattern of mammalian tissue using a spot size of 2.5-mm with power settings and pulse durations sufficient to bring the surface temperature to 100°C. Nd:YAG, 80 W for 1.5 s, ARG, 8 W for 0.31 s, CO_2, 1 W for 0.28 s.

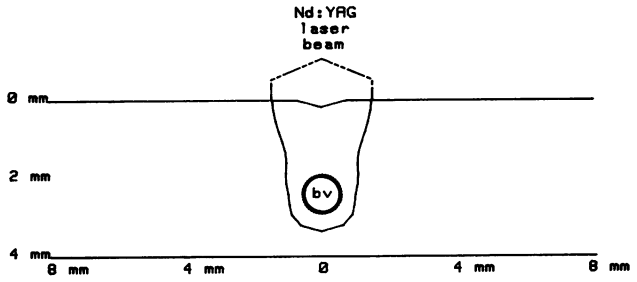

FIGURE 5 Theoretical heating pattern of tissue containing a blood vessel (bv) of 1-mm diam. using the Nd:YAG laser at a power setting of 80 W and a single-pulse duration of 1 s. Plotted are the 60 and 100°C isotherms, representing tissue coagulation and vaporization, respectively. Only a small area at the tissue surface reached 100°C.

tissue effects have been described extensively in the medical literature (13, 14). Comparison of histological observations indicate that the current model provides a reasonable approximation of the size and shape of these lesions throughout a wide range of power settings. Examples of such computations for the Nd:YAG, Argon, and CO_2 lasers are represented in Fig. 4. These three lasers are currently used in clinical medicine.

The "cell method" of computation used in our model is particularly useful in simulating the regional and temperature-dependent variations of absorption and scattering that frequently occur in biological tissues. In Fig. 5 the 60°C isothermal plot is distinctly altered by the presence of a blood vessel, here artificially represented by several "cells" of increased absorption and decreased scattering. The directional heat sink effect of blood flowing within the vessel can also be easily represented when the two-dimensional numerical matrix is expanded to three dimensions.

DISCUSSION

The theoretical model presented in this paper has been demonstrated to provide a sensitive and reasonably accurate approximation of the pattern of heating within biological tissue undergoing laser irradiation. This model accounts for the heterogeneity found within biological tissues. However, the formulae as described above are based on cylindrical symmetry and are therefore somewhat limited in their ability to represent the three-dimensional asymmetry of tissue. Maximal utilization of the model requires a three-dimensional numerical array format that should be the basis of future applications of this model. One such application, in preparation, will quantitatively relate these theoretical considerations to actual clinical technique. Therapeutic effectiveness will undoubtedly be enhanced by such correlations.

The authors would like to thank Dr. G. Benedek for helpful comments, and Dr. E. Sacks for the use of his computer.

This paper was supported in part by a grant from the National Science Foundation.

Received for publication 20 March 1982 and in final form 1 September 1982.

REFERENCES

1. Kiefhaber, P. N., G. Nath, and K. Moritz. 1977. Endoscopical control of massive gastrointestinal hemorrhage by irradiation with a high-power Neodymium-YAG laser. *Prog. Surg.* 15:140.
2. Auth, D. C. 1981. Endoscopic Control of Gastrointestinal Hemorrhage. J. P. Papp, editor. CRC Press, Boca Raton, FL. 75–86.
3. Regan, J. D., and J. A. Parrish, editors. 1980. The Science of Photomedicine. Plenum Publishing Corp. New York.
4. Anderson, R. R., and J. A. Parrish. 1981. Microvasculature can be selectively damaged using dye lasers: a basic theory and experimental evidence in human skin. *Lasers Surg. Med.* 1:263.
5. Hofstetter, A., and F. Frank. 1980. The Neodymium-YAG Laser in Urology. Hoffman–La Roche & Co., Basel, Switzerland.
6. Hansen, W. P. R. J. Greeenwald, and H. F. Bowman. 1974. Application of the CO_2 laser to thermal properties measurements in biomaterials. *Trans.ASME.* H96:2138.
7. Halldorsson, T., and J. Langerholc. 1978. Thermodynamic analysis of laser irradation of biological tissue. *Appl. Opt.* 17:3948.
8. Halldorsson, T. W. Rother, J. Langerholc, and F. Frank. 1981. Theoretical and experimental investigations prove Nd:YAG laser treatment to be safe. *Lasers Surg. Med.* 1:253–262.
9. Kovtun, A. V. V. S. Kondratyev, and D. V. Terekhov. 1980. Experimental determination of the absorption coefficients of biological tissues. *Biophysics (Engl. Transl. Biofizika.).* 25:1092.
10. Bellina, J. H., and Y. J. Seto. 1980. Pathological and physical investigations into CO_2 laser-tissue interactions with specific emphasis on cervical intraepithelial neoplasm. *Lasers Surg. Med.* 1:47.
11. Langerholc, J. 1979. Moving phase transitions in laser-irradiated biological tissue. *Appl. Opt.* 18:2286.
12. Mihalas, D. 1980. Stellar Atmospheres. Freeman & Company, Inc.
13. Johnston, J. H., D. M. Jensen, W. Mautner, and J. Elashoff. 1980. YAG laser treatment of experimental bleeding canine gastric ulcers. *Gastroenterology.* 79:1252.
14. Silverstern, F. E., D. A. Gilbert, A. V. Feld, and R. L. Protell. 1981. Endoscopic Control of Gastrointestinal Hemorrhage. J. P. Papp, editor.CRC Press, Boca Raton, FL. 87–102.